

# Force extension curves for polymers with hydrophobic patches: Role of Disorder

Ankur Mishra,<sup>1</sup> Ajay S. Panwar,<sup>1,\*</sup> and Buddhapriya Chakrabarti<sup>2,†</sup>

<sup>1</sup>*Department of Metallurgical Sciences, Indian Institute of Technology, Mumbai, INDIA.*

<sup>2</sup>*Department of Mathematical Sciences, Durham University, Durham, DH1 3LE, UK.*

(Dated: July 2, 2012)

Motivated by single molecule experiments on biopolymers we explore force vs. extension behavior of flexible chains with hydrophobic segments using numerical simulations and theory. We find that in addition to the fraction of hydrophobic patches their spatial distribution along the backbone of the chain play a major role in altering its mechanical response. These results are discussed in light of the helix-coil model for biopolymers.

PACS numbers:

## INTRODUCTION

Biopolymers such as DNA, RNA, and proteins carry out a majority of cellular processes that are crucial to sustaining life[1]. These processes are often associated with conformational changes of biomolecules. Several single molecule experiments, that probe mechanical properties of biomolecules, aim to relate primary structure to their native conformation and hence function[2].

Theoretical investigations on mechanical properties of proteins, DNA and other bio-macromolecules often use coarse-grained descriptions modeling structural components as non-linear elastic springs. Sequence heterogeneities are manifested as stiff and compliant elements along the chain backbone and are modeled by a site dependent bending modulus  $\kappa_i$  (where  $i$  corresponds to the lattice site). Statistical mechanical techniques rooted in the helix-coil model [3] and the worm-like chain model [4, 5] have been employed to explore stretching and bending response of biopolymers [6, 7]. These models however assume an annealed form of disorder, allowing for the interconversion between the “helix” and “coil” phases of the polymer chain as a function of either temperature or force. How does the mechanical response of a polymer chain with quenched disorder differ from that of an annealed one?

Motivated by this question we explore the mechanical properties of a polymer chain with hydrophobic and hydrophilic beads representing the quenched disorder using Langevin dynamics simulations and theory. We investigate the stretching response of a polymer subject to equal and opposite tensile forces applied to its ends. In our simulations the polymer chain is composed of hydrophobic and hydrophilic segments with the ability to self-hybridise. Our main result is that the mechanical response of the polymer chain is determined both by the fraction of hydrophobic contacts,  $f$ , as well as their arrangement along the chain backbone. We consider three disorder configurations: (a) random, corresponding to hydrophobic segments uniformly distributed throughout the chain backbone, (b) periodic, where a repeat unit of hydrophobic beads are interspersed with hydrophilic

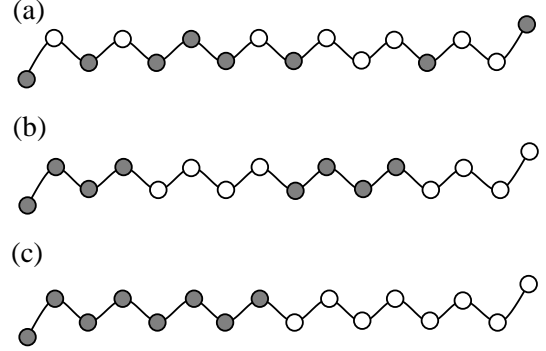


FIG. 1: Schematic representation showing hydrophobic groups (black circles) arranged along the chain backbone in (a) random, (b) periodic, and (c) block copolymer arrangements respectively. The fraction of hydrophobic beads is  $f = 0.5$ .

ones at regular intervals, and (c) block copolymer, where the hydrophobic groups are clumped together at one end of the chain. A schematic representation is shown in Figure 1 and the stretching response of different configurations are shown in Figure 3.

Khokhlov and co-workers have investigated *de novo* protein design of  $A - B$  copolymers that give rise to folded configurations [8–15]. The goal of this study was to identify arrangements of  $A$  and  $B$  molecules on the chain backbone that gives rise to globular states akin to native protein conformations. In order to investigate this a bead-spring polymer is equilibrated in a poor solvent forming a globule. The atoms that form the core shell of this globular structure are “colored” [10, 11] and the chain is stretched out to note the position of these atoms along the chain backbone. A set of backbone atom arrangements that lead to optimal packing geometries can then be identified. However the mechanical response of chains with imposed quenched disorder to an applied tensile force has not been explored.

Our results can be summarized as follows: we observe a sharp first order transition in the chain size at a critical force  $F_c$  for all three disorder realisations at a high value of the hydrophobic bead fraction  $f$  (see figure 3).

For a fixed hydrophobic fraction  $f$  (and  $f > 0.5$ ) the critical force  $F_c$  for the block copolymer distribution is observed to be higher than that of the periodic and random distribution. Interestingly, the difference between the critical forces corresponding to periodic and random distributions is negligible. The second result is that the critical force is zero for all three distributions for low values of  $f$ . A non-zero critical force  $F_c$  is observed above a threshold value of  $f$  which is found to be the same for all three distributions. The nature of the transition is first order like for block copolymer distribution whereas appears to be a crossover phenomena for the random and periodic ones.

## SIMULATION METHOD

The co-polymer is modeled as a freely-jointed bead-spring chain consisting of  $N$  beads linearly connected by  $N - 1$  springs. The co-polymer comprises of two types of monomers (or beads), they are either hydrophobic or hydrophilic. In stating the extent of hydrophobicity of the monomers, we are emphasizing the relevance of our coarse-grained simulations to dilute solutions of polymers in an aqueous solvent. As illustrated in Fig. 1, we consider three different arrangements of hydrophobic beads along the polymer chain. The hydrophobic beads are distributed either in a random, periodic or block co-polymer arrangements. Figure 1 represents the three different distributions for a chain with a fraction,  $f = 0.5$ , of hydrophobic groups.

Each bead in the polymer chain represents a Brownian particle, and the length of each link (spring) corresponds to the Kuhn length,  $l_0$ , for the polymer. The dynamics of each bead is described by the Langevin equation,

$$m_i \frac{d^2 \mathbf{r}_i}{dt^2} = -\zeta \mathbf{v}_i - \nabla_i U(r_{ij}) + \mathbf{F}_i^r(t) + \mathbf{F}_i^{ext}, \quad (1)$$

where  $m_i$ ,  $\mathbf{r}_i$  and  $\mathbf{v}_i$  represent the mass, position and velocity of particle  $i$ , respectively. The random force,  $\mathbf{F}_i^r(t)$ , arising from the bombardment of the monomer bead by the solvent molecules is described by the fluctuation-dissipation theorem,

$$\langle \mathbf{F}_i^r(t) \mathbf{F}_j^r(t') \rangle = 6\zeta k_B T \delta(t - t') \delta_{ij}, \quad (2)$$

where  $k_B$  is the Boltzmann constant,  $T$  the absolute temperature, and  $\zeta$  is the frictional drag. Externally applied, equal and opposite forces,  $F_i^{ext}$ , act on the terminal beads of the chain. However,  $F_i^{ext} = 0$  for the remaining polymer beads. Equation 1 was solved numerically using the velocity-Verlet algorithm, with a time step  $\Delta t = 0.001\tau$ , where  $\tau = l_0(m/\epsilon_{LJ})^{1/2}$ .

The net interaction potential,  $U(r_{ij})$ , is given by,

$$U(r_{ij}) = U_{LJ} + U_{bond}, \quad (3)$$

corresponding to the excluded volume interactions and bond stretching, respectively. The excluded volume interaction between any two beads is described by,

$$U_{LJ}(r_{ij}) = \begin{cases} 4\epsilon_{LJ}[(\sigma/r_{ij})^{12} - (\sigma/r_{ij})^6], & r_{ij} \leq 2.5\sigma, \\ 0, & r_{ij} > 2.5\sigma, \end{cases} \quad (4)$$

where  $r_{ij} = |\mathbf{r}_i - \mathbf{r}_j|$ ,  $\epsilon_{LJ}$  is the Lennard-Jones interaction parameter and  $\sigma$  is the bead diameter. In our simulations, we have set the bead diameter  $\sigma = 0.75l_0$  [16]. We use  $\epsilon_{LJ}$ ,  $l_0$  and  $m$  as scales for energy, length, and mass, respectively. The mass of a polymer bead is set to a value of one. The bond stretching potential between adjacent beads is given by the FENE potential,

$$U_{bond}(r_b) = -\frac{1}{2}kr_b^2 \ln \left[ 1 - (r_b/R_{max})^2 \right], \quad (5)$$

where  $r_b$  is the separation distance between adjacent beads,  $R_{max} = 1.5l_0$  is the maximum allowable separation distance between bonded beads and  $k$  is the spring constant. The simulations were executed in the open-source molecular dynamics simulation package LAMMPS[17].

We used a chain size of  $N = 100$  in our simulations. The polymer chain is enclosed inside a cubic box of edge length  $50 l_0$  with periodic boundary conditions imposed in all three directions. In order to model the appropriate effective solvent interactions, we set  $\epsilon_{LJ} = 1.5$  for the hydrophobic beads and  $\epsilon_{LJ} = 0.1$  for the hydrophilic ones. For a homopolymer, a choice of  $\epsilon_{LJ} = 0.1$  for all beads simulates a polymer chain that demonstrates self-avoiding walk statistics, whereas a value of  $\epsilon_{LJ} = 1.5$  results in a collapsed globule. When  $\epsilon_{LJ} = 0.4$ , we recover Gaussian statistics for the homopolymer. We varied the hydrophobic bead fraction,  $f$ , between 0 and 1, to explore the effects of disorder on the force-extension response of the polymer chain.

The initial configuration of the chain was such that a fraction,  $f$ , of the beads were assigned as hydrophobic and the rest,  $1 - f$ , were considered to be hydrophilic. Initially, the polymer chain is equilibrated in solution for a period of  $4 \times 10^6$  time steps in the absence of any external force ( $F^{ext} = 0$ ). The chain was then stretched from the equilibrium state to full extension by an incremental increase in pulling force,  $F^{ext}$ , from a value of 0.1 to 10. The pulling cycle is followed by a retraction cycle where  $F^{ext}$  is decreased from 10 to 0.1. During the pulling and the retraction cycles, the polymer is equilibrated for a period of  $5 \times 10^6$  time steps at a given value of  $F^{ext}$ . We calculate the time-averaged value of the radius of gyration,  $R_g$ , over the equilibration period. Consequently, the extension of the polymer at that value of applied force is calculated. The data was averaged over  $N_{run} = 5$ ,

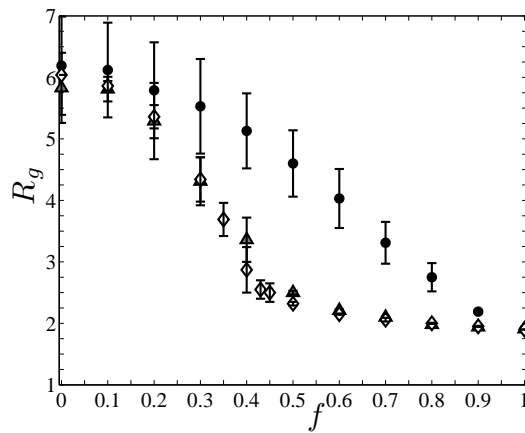


FIG. 2: Figure shows the average radius of gyration  $\langle R_g \rangle$  over different disorder realisations as a function of the hydrophobic groups for (a) block copolymer (filled circles  $\circ$ ), (b) periodic distribution (filled triangles  $\triangle$ ), and random distribution (open diamonds  $\diamond$ ). The average is over 5 different realisations for the random system.

disorder realizations for the three types of distributions and each value of  $f$ . In the case of the random distribution, the five realizations correspond to five statistically different arrangements of hydrophobic groups along the polymer backbone, for the same value of  $f$ . The results obtained from these different realizations were used to calculate the average values of and standards for and corresponding to a particular value of force and fraction of hydrophobic groups

## RESULTS AND DISCUSSION

Figure 2 describes the variation of the radius of gyration of the polymer,  $R_g$ , as a function of  $f$ , for all three distributions at zero applied force. We find that as  $f$  increases,  $R_g$  decreases monotonically for all three cases. An increase in  $f$  results in aggregation of hydrophobic groups leading to a monotonic decrease in  $R_g$ . The variation of  $R_g$  with  $f$  follows near identical trends for both the random and periodic distributions for the entire range of  $f$ . Both distributions display a sigmoidal behavior, where the polymer chains show a transition from a coiled state to a collapsed, globular state for  $f > 0.4$ . This is in contrast to the behavior of  $R_g$  with  $f$  for the block copolymer distribution. For  $f \lesssim 0.2$ ,  $R_g$  values for the block copolymer distribution are close to the ones corresponding to the periodic and random ones. However, for  $0.2 \lesssim f \lesssim 0.8$ , the rate of change of  $R_g$  with respect to  $f$  is lower than the other two distributions. Also, the block copolymer does not go through a sharp phase transition as the other two distributions. For  $f \gtrsim 0.8$ ,  $R_g$  values for all three distributions tend to a common value. At  $f = 1.0$ ,  $R_g$  is the same for all three distributions.

In the case of a block copolymer, the hydrophobic groups at one end form a globule, while the rest of the chain assumes a coil structure. As  $f$  increases, a greater fraction of the chain is in the globular state, whereas the hydrophilic block remains as a coil. Consequently, the entire chain does not form a compact globule for any value of  $f$  apart from  $f = 1$ . However, for the periodic and random distributions, hydrophobic groups are distributed along the entire polymer chain, which enables attractive interactions between hydrophobic groups that are far separated along the chain contour. This results in a first order coil-to-globule transition for  $f \approx 0.35$ .

Figure 3 shows extension,  $\langle R^2 \rangle^{1/2}/L$ , vs. force,  $F$ , for all three distributions at four different hydrophobic fractions  $f = 0.2, 0.4, 0.6$  and  $0.8$ . For small hydrophobic fraction,  $f = 0.2$  (Fig. 3(a)), the chain extension increases monotonically with  $F$  for all three distributions, with little variation between them. For higher hydrophobic fractions ( $f = 0.4, 0.6, 0.8$ ), a first order globule to coil transition is observed at a critical force,  $F_{cr}$ . In the case of periodic and random distributions, the hydrophobic groups, which are distributed along the entire chain contour, hybridize with each other to form a compact globule. Therefore, when the magnitude of the applied force is small, the globule is only slightly distorted from its equilibrium conformation. Consequently, the extension remains nearly constant for small  $F$ . In contrast, the block copolymer undergoes a relatively larger extension for smaller values of  $F$  ( $F < F_{cr}$ ) for  $f = 0.4, 0.6, 0.8$ . This is because in poor solvents, the block copolymer consists of a hydrophobic globule at the end of a flexible, hydrophilic coil that is easy to stretch under the application of a tensile force. Once the long wavelength fluctuations along the chain backbone have been smoothened out, the end-to-end distance of the chain remains constant upon an increase in the force  $F$ . However, beyond the critical force  $F_{cr}$ , the chain unravels undergoing a jump discontinuity in size. On further increase in  $F$  above  $F_{cr}$ , the chain stretches out to full extension. As is expected, the large force behavior is identical for different disorder realisations as shown in Fig. 3.

Figure 4 shows the variation of  $F_{cr}$  as a function of  $f$  for all three distributions of hydrophobic groups. For  $f < 0.3$ , the critical force,  $F_{cr}$ , required to uncoil the polymer chain is zero for all three distributions. This is because for small  $f$ , the total number of hydrophobic contacts are few. Thus, the polymer remains in a coil-like state, and starts stretching continuously even for small values of  $F$ . In case of the block copolymer,  $F_{cr}$  increases discontinuously to a large value of approximately 3.2 (from a zero value) for  $f \approx 0.35$ , and with increasing  $f$ ,  $F_{cr}$  quickly saturates to a value of 4.0. In contrast, for the periodic and random distributions,  $F_{cr}$  appears to increase linearly with  $f$  for  $f \gtrsim 0.35$ . It is interesting to note that the  $F_{cr}$  vs.  $f$  curves are nearly identical

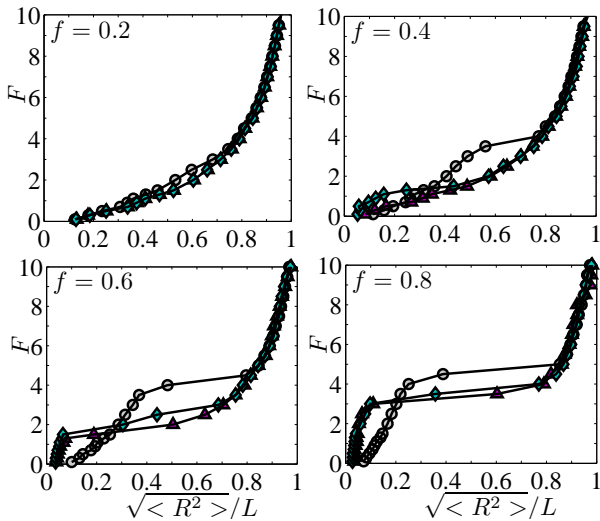


FIG. 3: Figure showing force  $F$  vs. extension  $\langle R_g \rangle/L$  for different values of the hydrophobic fraction  $f$  and different disorder realisations along the chain backbone, block copolymer (filled circles  $\circ$ ), periodic (triangles  $\triangle$ ), and random distribution (diamonds  $\diamond$ ).

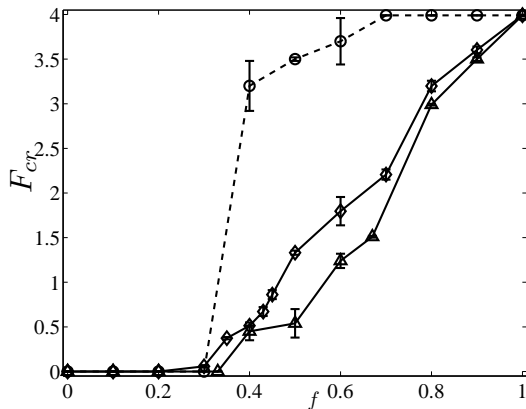


FIG. 4: Figure shows the variation of critical force  $F_{cr}$  as a function of the fraction of hydrophobic groups  $f$  for different disorder realisations (a) block copolymer (circles  $\circ$ ), (b) periodic distribution (triangles  $\triangle$ ), and random distribution (diamonds  $\diamond$ ). The average is over 5 different realisations for the random system.

for the random and periodic distributions. For  $f = 1$  the critical force of uncoiling  $F_{cr} = 4$  (in dimensionless units) is same for all three distributions. This is because all three distributions have the same structure when all the beads are hydrophobic.

## SUMMARY

We have utilized Langevin dynamics simulations to investigate the force vs. extension behavior of a single co-polymer composed of hydrophobic and hydrophilic

groups arranged in periodic, random and block distributions along its backbone. Our simulations demonstrate that the mechanical response of a heteropolymer undergoing a force-induced globule-coil transition is dependent on the distribution of hydrophobic groups along its backbone. All three disorder realizations form globular structures at large hydrophobic fractions, and show a first order transition in their sizes at a critical force,  $F_c$ . However, for a given fraction, the critical force is observed to be higher for the block copolymer in comparison to the periodic and random distributions. In addition, our simulations show that the force-extension responses of the periodic and random distributions are nearly identical. From the force-extension curves, we plotted the critical force,  $F_c$ , as a function of the hydrophobic fraction,  $f$ . Since the polymers behave like coils for small hydrophobic fractions,  $F_c = 0$  for all three distributions. An important result is that  $F_c$  is non-zero for  $f \approx 0.35$  for all three distributions. On further increase in the hydrophobic fraction, the critical force shows a first order transition for the block copolymer. However, it increases continuously for the random and periodic distributions. Interestingly, we again note that the transition behaviors of the random and periodic distributions are nearly identical.

We now place our results in context of existing theories on the subject. The collapse transition of disordered polymers has been the subject of several studies [19–21]. Statistical techniques rooted in replica methods has been used to explore globular conformations [22] (and references therein). Further optimal distributions of hydrophobic and hydrophilic groups along the primary sequence leading to folded conformations have been investigated in context of rational design of proteins [8–15, 18]. and statistical mechanical theories of random systems [19, 21] have been employed to explore such conformational states of A-B/H-P heteropolymers.

However mechanical behavior of disordered polymers have been less investigated [23]. Our results illustrate the difference in mechanical properties of such heteropolymers having similar bulk structural properties but differing in the local arrangement of disorder undergoing a force induced globule-coil transition. Transfer matrix calculations based on the helix-coil model for annealed disorder [6, 7] can be adapted to the case of quenched disorder. However this is omitted from the present paper for brevity and the fact that it does not yield to any new insights over those obtained from simulations.

We hope that this work will spark interest amongst polymer chemists interested in rational design of polymers that aim to identify sequences that lead to specific folded structures. Further, we believe this work would also be useful to single molecule biophysicists interested in understanding protein conformational transitions and allostery.

- 
- \* Electronic address: panwar@iitb.ac.in  
† Electronic address: buddhapriya.chakrabarti@durham.ac.uk
- [1] B. Alberts, A. Johnson, J. Lewis, M. Raff, K. Roberts, and P. Walter, *Molecular Biology of the Cell*, Garland, New York (2002).
  - [2] C. Bustamante, W. Cheng, and Y. X. Mejia, *Cell*, **144**, 480 (2011).
  - [3] D. Poland, and D. Scheraga, *Theory of Helix-Coil transitions in biopolymers: statistical mechanical theory of order-disorder transition in biological macromolecules*, Academic Press (1970).
  - [4] M. E. Fisher, *Am. J. Phys.* **32**, 343 (1964).
  - [5] J. Marko, and E. Siggia, *Macromol.* **28**, 8759 (1995).
  - [6] B. Chakrabarti, and A. J. Levine, *Phys. Rev. E* **71**, 031905 (2005).
  - [7] B. Chakrabarti, and A. J. Levine, *Phys. Rev. E* **74**, 031903 (2006).
  - [8] A. V. Chertovich, V. A. Ivanov, A. A. Lazutin, and A. R. Khokhlov, *Macromol. Symp.* **160**, 41 (2000).
  - [9] Y. A. Kriksin, P. G. Khalatur, and A. R. Khokhlov, *Macromol. Theory Simul.* **11**, 213 (2002).
  - [10] E. A. Zheligovskaya, P. G. Khalatur, and A. R. Khokhlov, **59**, 3071 (1999).
  - [11] A. R. Khokhlov, and P. G. Khalatur, *Phys. Rev. Lett.* **82**, 3456 (1999).
  - [12] J. M. P. van den Oever, *et al.* **65**, 041708 (1999).
  - [13] A. V. Berezkin, P. G. Khalatur, and A. R. Khokhlov, *J. Chem. Phys.* **118**, 8049 (2003).
  - [14] A. R. Khokhlov, and P. G. Khalatur, *Curr. Opin. Solid State Mater. Sci.* **8**, 3 (2004).
  - [15] A. V. Chertovich, E. N. Govorun, V. A. Ivanov, P. G. Khalatur, and A. R. Khokhlov, *Eur. Phys. J. E* **13**, 15 (2004).
  - [16] S. Liu, and M. Muthukumar, *J. Chem. Phys.*, **116**, 9975 (2002).
  - [17] S. J. Plimpton, *J. Comp. Phys.*, **117**, 1 (1995), <http://lammmps.sandia.gov>.
  - [18] K. F. Lau, and K. A. Dill, *Macromol.* **22** 3986 (1989).
  - [19] A. Yu Grosberg, *J. Stat. Phys.*, **38**, 149 (1985).
  - [20] S. P. Obukhov, *J. Stat. Phys.*, **19**, 3655 (1986).
  - [21] T. Garel, L. Leibler, and H. J. Orland, *J. Physique II*, **4**, 2139 (1994).
  - [22] V. S. Pande, A. Yu Grosberg, and T. Tanaka, *Rev. Mod. Phys.*, **72**, 259 (2000).
  - [23] D. Bensimon, D. Dohmi, and M. Mezard, *Europhys. Lett.*, **42**, 97 (1998).